Communication

Stable Triple-Wavelength Random Fiber Laser Based on Fiber Bragg Gratings

Airull Azizi Awang Lah [1], Abdul Hadi Sulaiman [2], Fairuz Abdullah [2], Sumiaty Ambran [1], Eng Khoon Ng [3], Mohammed Thamer Alresheedi [4], Mohd Adzir Mahdi [5,*] and Nelidya Md Yusoff [6,*]

[1] Malaysia–Japan International Institute of Technology, University of Technology Malaysia, Jalan Sultan Yahya Petra, Kuala Lumpur 54100, Malaysia; aazizi9@graduate.utm.my (A.A.A.L.); sumiaty.kl@utm.my (S.A.)

[2] Institute of Power Engineering, Universiti Tenaga Nasional, Jalan IKRAM-UNITEN, Kajang 43000, Selangor, Malaysia; abdulhadi@uniten.edu.my (A.H.S.); fairuz@uniten.edu.my (F.A.)

[3] Department of Engineering, University of Cambridge, Cambridge CB3 0FA, UK; ekn27@cam.ac.uk

[4] Department of Electrical Engineering, College of Engineering, King Saud University, P.O. Box 800, Riyadh 11421, Saudi Arabia; malresheedi@ksu.edu.sa

[5] Wireless and Photonics Networks Research Centre, Faculty of Engineering, University of Putra Malaysia, Serdang 43400, Selangor, Malaysia

[6] Razak Faculty of Technology and Informatics, University of Technology Malaysia, Jalan Sultan Yahya Petra, Kuala Lumpur 54100, Malaysia

* Correspondence: mam@upm.edu.my (M.A.M.); nelidya.kl@utm.my (N.M.Y.)

Abstract: We demonstrate a generation of three lasing wavelengths with the assistance of Rayleigh backscattering as the stabilizer of peak power variations. The proposed laser consists of a combination of the semiconductor optical amplifier (SOA) and erbium-doped fiber amplifier (EDFA) as the amplifying media. Three fiber Bragg gratings are employed as the selective wavelength selectors at 1544, 1547 and 1550 nm. At 110 mA SOA current and 18 dBm EDFA output power, a flattened output spectrum with 0.9 dB peak power variation is attained. In terms of stability, the maximum peak power fluctuation for the individual laser is 0.24 dB within 120 minutes observation period. Without the Rayleigh backscattering effect, the peak power flatness is severely degraded. This shows that the weakly distributed photons can be utilized as peak power stabilizers in fiber laser systems.

Keywords: random fiber laser; semiconductor optical amplifier; erbium-doped fiber amplifier; fiber Bragg grating; intensity-dependent loss

1. Introduction

In recent years, multiwavelength fiber lasers have gained interest among researchers in optical fiber communication due to their application in wavelength division multiplexing systems. This technology enables a solitary optical fiber to carry several signals simultaneously at different wavelengths, thereby increasing the bandwidth capacity. Besides optical communications [1], it also has potential use as a sensing application in sensor and in strain measurement [2] and spectroscopy [3]. Normal lasers are based on a well-defined energy level, require external reflection for feedback, show strong coherence, and operate in specific gain media [4]. On the other hand, random lasers use scattering-disordered media for feedback, have low coherence, and do not depend on external mirrors for feedback as light is amplified by the Rayleigh scattering feedback in the resonator [5].

In the fiber laser scope, random fiber lasers (RFLs) have been the subject of intense research and have received considerable attention due to their unique characteristics. They offer design simplicity over traditional laser technology, while also displaying desirable qualities of a laser such as high efficiency and good directionality [6]. Therefore, this class of laser has vast potential in the industry such as optical communication [7], geophysical field [8], biomedical [9], electronic applications [10], and imaging applications [11]. RFL is

one of the attractive solutions for sensing elements in long-distance fiber, such as oil and gas, and power transmission lines [8].

To construct RFLs, a very long section of optical fibers in the order of tens of kilometers is normally employed. Owing to this nature, according to [6], there are three scattering categories involved in the lasing process: stimulated Raman scattering (SRS) [12], stimulated Brillouin scattering (SBS) [13], and Rayleigh backscattering (RBS) [14]. SRS is the main phenomenon for light amplification along the optical fibers. On the other hand, the SBS effect has emerged as a limiting factor to achieve a stable random laser. This is normally observed during the stochastic period just before the initiation of a broad spectrum of lasers. While the effect of RBS is crucial as a distributed reflector in the light waveguiding medium. Although it is a random process, when the light propagation principle in optical fibers is obeyed, then it can be a positive effect in RFLs. However, the RBS effect is very weak and requires a huge amount of Raman amplification in order to be effective. In addition to this, Raman amplification in RFL requires high excitation power for lasing actions to take place. Owing to this drawback, it is noteworthy to find alternative solutions for amplifying light in RFL systems.

Two widely used optical amplification technologies are the erbium-doped fiber amplifier (EDFA) and semiconductor optical amplifier (SOA). EDFA is frequently preferred over SOA due to the higher-saturated output power and lower-lasing threshold [14]. Despite these advantages, EDFA operates as a homogenous medium at room temperature, leading to mode competition that can cause lasing instability and restrict the number of possible lasing signals. Conversely, SOA is naturally inhomogeneous and is efficient in suppressing the mode competition as a result of stable multiple lasing lines generated simultaneously [15]. Only a few articles have reported on the RFL using SOA as the gain media, to date. H. Shawki et al. [16] utilized RBS in single-mode fiber (SMF) to achieve a laser that operates in a single longitudinal mode with a narrow linewidth. On the other hand, Y. Xu et al. [17] demonstrated a 1 kHz narrow linewidth dual-wavelength SOA-based RFL. In both works, two gain media were employed to compensate for the large loss and amplify the weak RBS feedback in the ring cavity. P. Tovar et al. demonstrated that single-mode operation dominated when the SOA input current was close to the threshold value and increasing the SOA current resulted in multimode operation [18]. A hybrid configuration of gain media has been explored, aiming for new sensing applications, lower noise, and higher RFL efficiency [5]. RFLs that operate on hybrid gain media have been reported to use Brillouin–Raman [19], Brillouin–erbium [20], Raman–erbium [21], and SOA–EDFA [22]. In [22], the proposed setup required an additional electronic components to adjust the cavity length and increased the lasing magnitude.

The generation of multiwavelength random fiber lasers (MWRFLs) relies not only on the gain medium, but also on the essential function of a comb filter. The comb filters that are usually used in MWRFL are the Sagnac loop mirror [23,24], Fabry–Perot filter [25–27], Lyot filter [28], and Mach Zehnder interferometer [29]. A few works of MWRFL have been published using fiber Bragg gratings (FBGs) as the comb filter, making it one of the most preferred comb filters among researchers [14,26,30,31]. Moreover, the maturity of FBG fabrication has led to its adoption in laser technologies, facilitating the creation of compact, inexpensive, and reliable fiber lasers [5].

Previously, several works in RFL were realized using FBGs as the selective wavelength filters. The study by T. Feng et al. [14] successfully produced six simultaneous lasers using an erbium-doped fiber laser based on RBS effect. A narrow linewidth dual-wavelength RFL was demonstrated by Y. Xu et al. [17] using two SOAs in a ring cavity. Researchers investigated the stability performance between SOA-based and EDFA-based RFLs. A work by P. Tovar et al. [18] studied the RFL mode operation according to SOA currents. Based on the reported work, the pulse operation mode is mainly a single mode, whereas at higher SOA currents, the operation mode shifts toward a multimode. Work by W. Zhang et al. [32] demonstrated that a lasing mode could be controlled by heating the FBG array locations in an EDFA-based RFL.

Most RFLs based on FBG were configured in a linear cavity [14,33–35] instead of a ring cavity [17,36]. However, the ring cavity's challenge is to produce simultaneous lasing signals due to its long cavity length [17,26,37]. This limitation leads to intense competition between the modes, mode-hopping, and the occurrence of multimode oscillations, which render the laser to be unstable and result in a broader linewidth. In this work, we have successfully demonstrated the high stability of triple-wavelength random fiber laser (TRFL) in a ring cavity based on EDFA, SOA, and FBG. This work uses the SOA and polarizer to solve the stability issue of RFL in a ring cavity. Another contributor to the high stability is due to the existence of RBS. The peak power stability of 0.11 dB is obtained in a 120 min observation period.

2. Experimental Setup

The experimental configuration of TRFL is illustrated in Figure 1. It is based on a ring cavity setup comprising two hybrid gain media (SOA and EDFA), 41 km long SMF, an isolator, a 10/90 splitter, a 50/50 coupler, two polarization controllers (PCs), three FBGs, polarization beam splitter (PBS), and four circulators. The SOA (Thorlabs, SOA1013S) operates from 1528 to 1562 nm wavelength range. To facilitate bidirectional amplification, the SOA is placed in between C1 and C2. The EDFA has 18 dBm of maximum output power which is controlled by its automatic power control mode. The EDFA comprises a forward-pumped configuration using a 300 mW laser diode at 980 nm wavelength. The length of erbium-doped fiber (Lucent HP980) is 17 m, which has a 5.3 dB/m absorption coefficient at 1550 nm, 8.2 µm mode filed diameter, 920 nm cutoff wavelength, and 0.18 numerical aperture. The SMF used is an ITU-T G.655 manufactured by the OFS (Truewave® RS Optical Fiber) to provide random distributed feedback in the laser cavity. The arrangement of the isolator allows the incident light to be dumped out. In this situation, only the RBS components generated in the SMF section to recirculate into the laser cavity through C3. These RBS components have weak signal strength which require an EDFA for amplifying their energy. The function of PC1 is to minimize any variation of laser performance due to the fluctuation of polarization states. On the other hand, PC2 induces the nonlinear polarization rotation (NPR) effect when combined with the PBS to achieve a flat output spectrum. Three FBGs at different wavelengths are spliced in series to reflect a triple-narrowband spectrum at 1544.03, 1547.13, and 1550.08 nm. The reflection bandwidths are characterized at 0.12 nm (FBG1), 0.10 nm (FBG2), and 0.11 nm (FBG3), respectively. The coupling of these reflected signals to the cavity is facilitated by C4. Another function of PBS is to split the light into two different routes at the orthogonal polarization states. Afterward, both separated lights travel to C1 and C2 before being bidirectionally amplified by SOA. After the amplification stage, both lights are combined by a 50/50 coupler. Finally, a splitter will tap out 10% of the lasing signal to an optical spectrum analyzer (OSA, Yokogawa AQ6370B). The remaining 90% of the lasing light remains in the cavity to make a complete roundtrip.
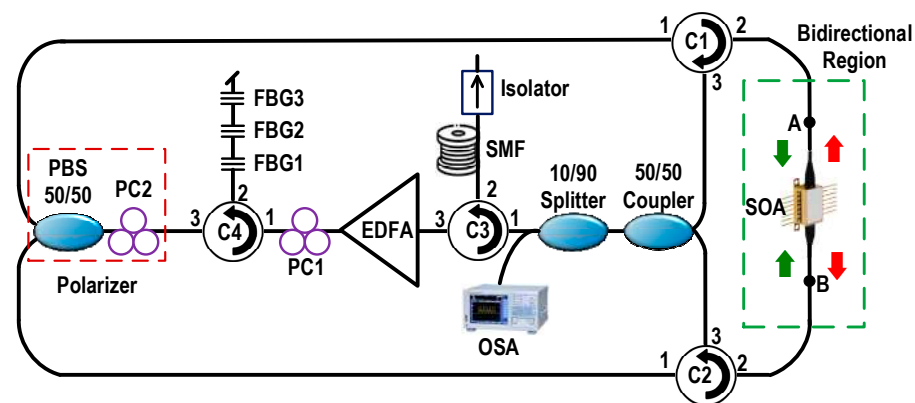

Figure 1. The experiment setup of TRFL using hybrid gain media and FBG.

Principle of Operation

The lasing wavelengths are determined by the selective filter characteristic of the FBGs. The SMF section provides RBS feedback of these circulating lights that maintain the phase coherence between the incoming and scattered light waves [17]. This coherent feedback requires a significant length of SMF, which occurs randomly in nature. Therefore, the random laser is built up by combining the coherent RBS in the SMF, round-trip amplification by the gain media and the FBG filtering effect.

Ring cavity has lower output power and side-mode suppression ratio (SMSR) compared to linear cavity [38]. Hence two gain media are used to improve the output power and SMSR. EDFA is a homogeneous gain medium and has strong mode competition. This heightens a tough challenge to achieve stable multiwavelength at room temperature [15]. To overcome this limitation, the EDF has to be immersed in liquid nitrogen [39] or have a specially designed twin-core EDF [40]. This creates complexity of operating and handling the laser cavity.

SOA has many advantages compared to the conventional EDFA due to its compactness, lower power consumption and inhomogeneous gain medium. It has the ability to suppress mode competition from the EDFA and generate flat and stable lasing lines [41]. Alongside that, the combination of SOA, PBS, and PC2 promotes an intensity-dependent loss (IDL) mechanism from the NPR effect [42]. The IDL is a phenomenon associated with the attenuation of the signal that is dependent on light intensity [15,42–44]. This mechanism is also used to mitigate the mode competition from the homogeneous gain medium broadening such as EDFA, and produce multiwavelength lasers with narrow wavelength spacing and good stability [45]. These SOA features are useful to complement the lasing performance provided by the EDFA alone.

3. Results and Discussion

This study explored the effect of an SOA current and PC1 plate rotations on the generated TRFL. It is expanded further to investigate the effect of RBS in TRFL stability, which is the main contribution in this study. The optical component parameter is fixed, except the PC1 plate and SOA current are varied to observe any flatness change at a maximum EDFA power of 18 dBm.

Figure 2a–d illustrates the TRFL output spectrum range from 1542 to 1552 nm at different SOA currents: 60, 80, 100, and 110 mA. PC1 is tuned for every SOA current value to optimize the lasing spectrum. Based on the experimental findings, the TRFL output spectrum consists of three lasing wavelengths of 1544, 1547, and 1550 nm. The highest peak power when the SOA input current is tuned to 60, 80, 100, and 110 mA is −66.8, −47.9, −36.9, and −33.2 dBm, respectively, as depicted in Figure 2a–d. It is important to note that the flatness of the TRFL output improves with the increment of the SOA current. Therefore, the best random lasing is attained at the SOA current of 110 mA with peak power flatness around 0.9 dB. As can be seen from the graphs, the TRFL spectrum exhibits higher output power with a higher SOA current. These relationships may explain that more energy is transferred to the amplified scattering photons at higher SOA currents, resulting in the total energy gain exceeding the total loss in the cavity. Meanwhile, the extinction ratio (ER) for SOA currents of 60, 80, 100, and 110 mA are 0.75, 13.87, 19.26, and 21 dB, respectively.

In continuation of Figure 2d above, each spectrum peak is magnified further to analyze the lasing bandwidth characteristics. Figure 3a–c depicts the 3 dB linewidth for each lasing line at the SOA current of 110 mA. The peak power is between −32.5 and −33.15 dBm, and the maximum ER is 22 dB. The 3 dB linewidth for the peak wavelength of 1544, 1547 and 1550 nm is 0.26, 0.25, and 0.25 nm, respectively. The 3 dB linewidth is narrower as compared to the FBG linewidth from the specification data sheet, which is 0.3 nm, due to the existence of RBS effect.
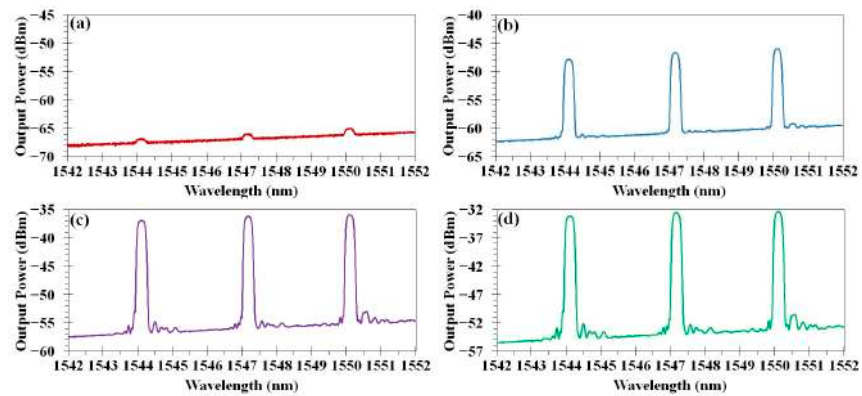
Figure 2. TRFL output power at SOA currents of (**a**) 60 mA, (**b**) 80 mA, (**c**) 100 mA, and (**d**) 110 mA.
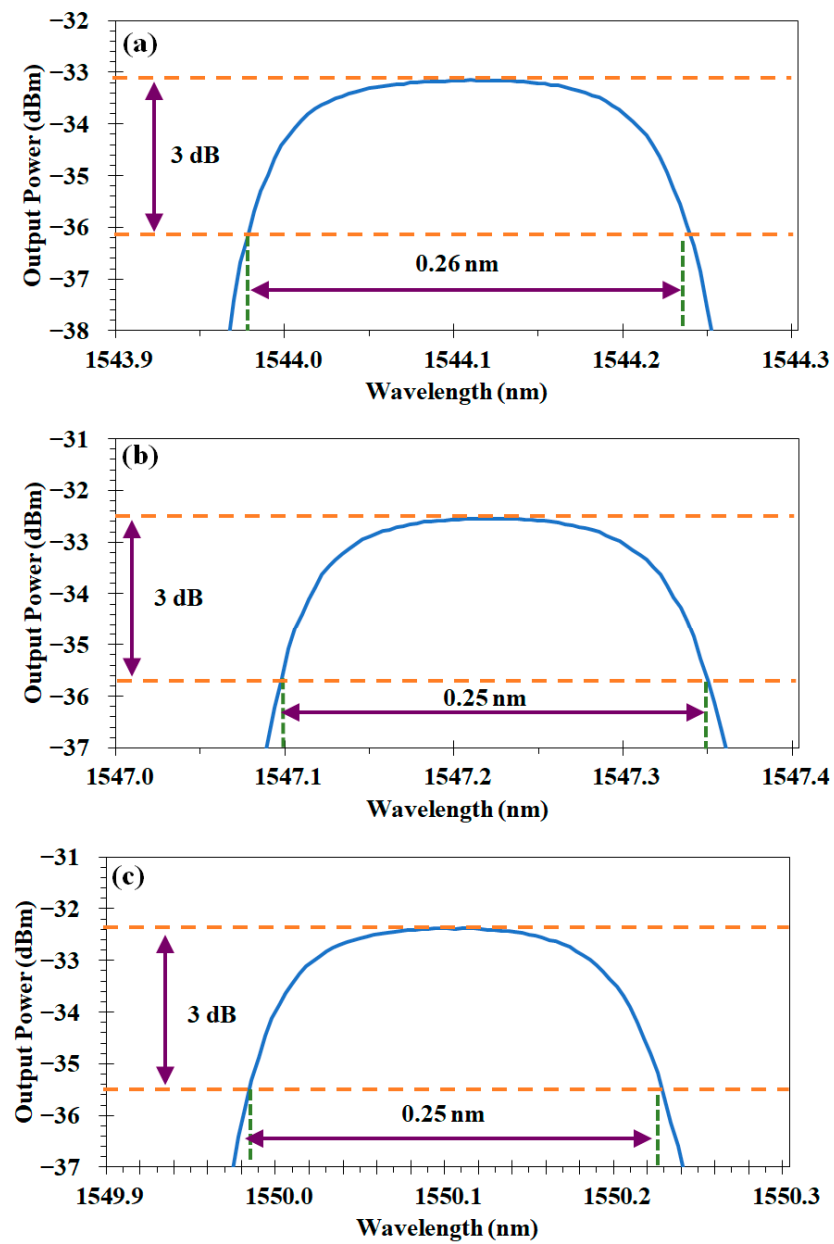

Figure 3. Lasing linewidth at the center wavelength of (**a**) 1544 nm, (**b**) 1547 nm, and (**c**) 1550 nm.

We investigated the effect of PC1 angle adjustment on the TRFL output power while maintaining other settings. The half-wave plate (HWP) angle of PC1 is varied in 20° intervals from 0° to 180°, and the experimental results are depicted in Figure 4a. Based on the findings, all measured spectra have similar patterns with no sign of significant fluctuations, regardless of the PC1 angle adjustment. This means that the change of the HWP angle of PC1 does not affect the TRFL output spectrum features due to the contribution of RBS and IDL mechanisms. Figure 4b depicts the peak power of the three center wavelengths at every HWP angle, according to Figure 4a. It is observed that the peak power of TRFLs at 1544, 1547, and 1550 nm lasing wavelengths are −34.0, −33.3, and −32.5 dBm, respectively, and the maximum peak power variation among these three lasers is only 1.5 dB. The RBS and bidirectional amplification in the SOA compensate the effect of the polarization-dependent loss in the cavity. The minor fluctuations in the peak power at higher wavelengths is attributed to higher reflectivity from the FBG [46].
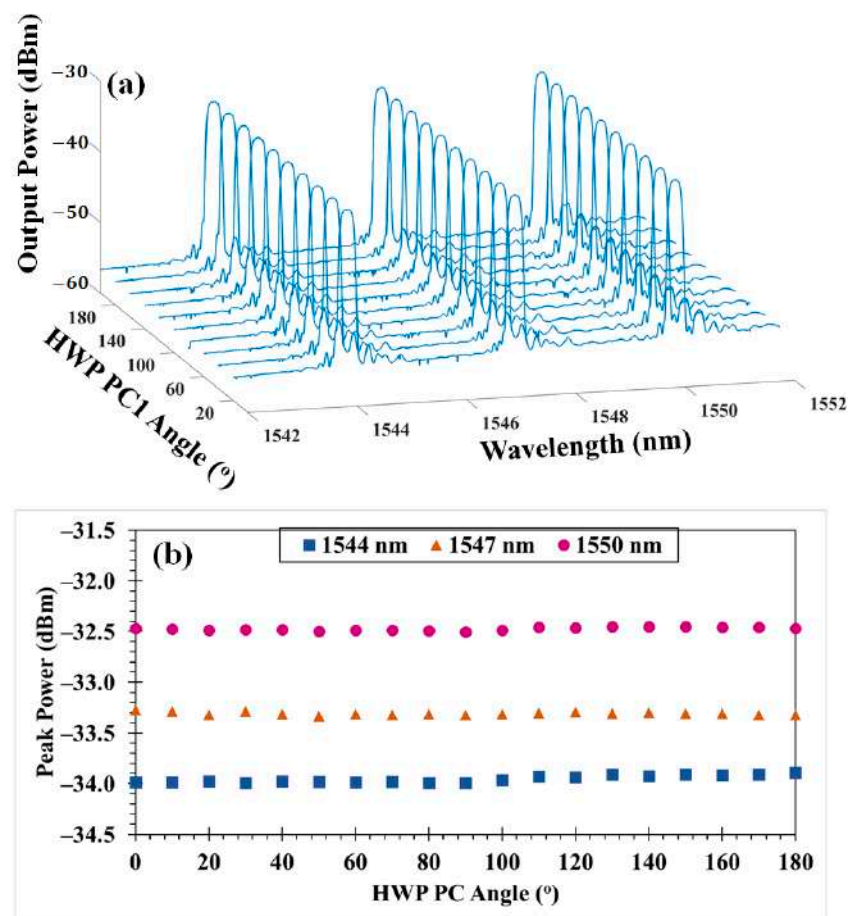

Figure 4. (**a**) The TRFL spectrum and (**b**) peak power at different HWP angles of PC1peak power at different HWP angles of PC1.

The investigation of the RBS effect on TRFL performance is achieved by analyzing the lasing spectrum with and without SMF in the experimental setup. Referring to Figure 1, the setup without SMF is obtained by removing the SMF together with C3 and the isolator. Thus, the 10/90 splitter is connected directly to the EDFA. The lasing spectrum for both conditions is illustrated in Figure 5, based on an SOA current of 110 mA. The peak power of TRFL with SMF is −33 dBm at the peak wavelengths of 1544, 1547, and 1550 nm. The similar peak power value at the three center wavelengths is proof that the three lasers are greatly flat. When the SMF is removed, the flatness is severely degraded, as the peak power variation of 44 dB is observed from this experiment. This significant finding proves that the RBS from the SMF is important to stabilize and flatten the peak power of TRFL.
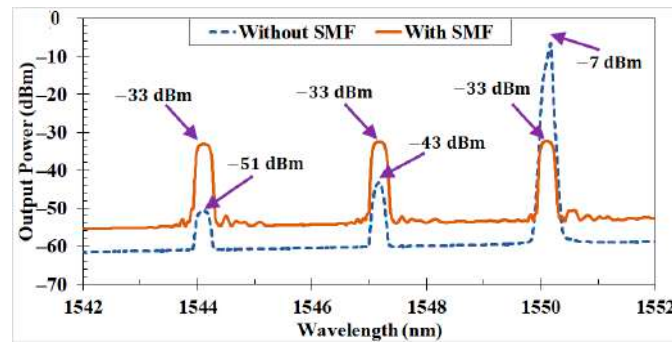
Figure 5. The peak power of TRFL, with and without SMF.

Stability of the TRFL output is investigated at the SOA input current of 110 mA, and the lasing spectrum data are captured every minute within two hours. Figure 6a shows the spectrogram of three lasing wavelengths at 1544, 1547, and 1550 nm within 120 min. Figure 6b illustrates the lasing stability as a two-dimensional coordinate. From these figures, there is no significant deviation of the output spectrum over the observation period. To analyze the fluctuation of the peak power and wavelength quantitatively, the value of these parameters is presented in Figure 6c,d. At 1544 nm lasing wavelength, the peak power variation is the lowest at 0.11 dB. The peak power differences at 1547 and 1550 nm are 0.24 and 0.20 dB, respectively. On the other hand, the maximum wavelength deviation among three lasing wavelengths is only 0.01 nm. The slight peak power deviations are influenced by the EDFA's mode competition. However, the SOA's inhomogeneous gain effectively reduces mode competition between lasing wavelengths, as a result of the flat-lasing spectrum. These results suggest that the generated TRFL has good stability in terms of peak power, with insignificant wavelength fluctuations.
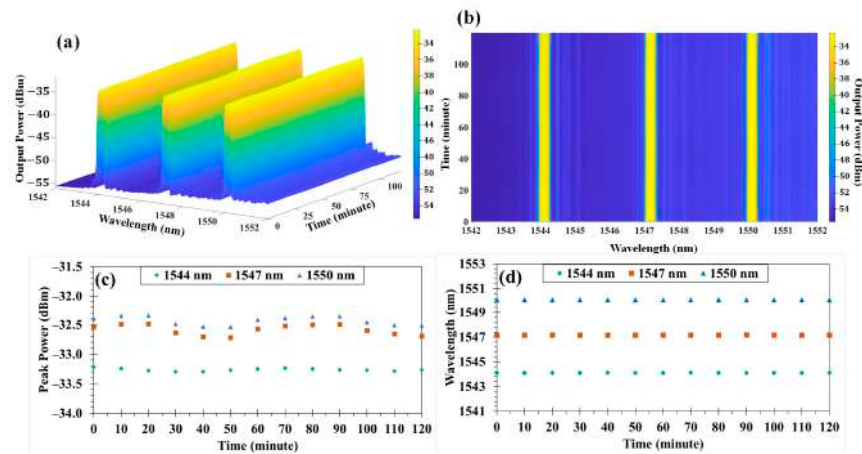

Figure 6. The stability result of the proposed TRFL within 120 min: (**a**) 3D spectrogram, (**b**) 2D spectrogram, (**c**) peak power fluctuations, and (**d**) lasing wavelength deviations.

4. Conclusions

We have successfully demonstrated a stable TRFL based on FBGs using hybrid gain media. The RBS from the SMF and IDL mechanism plays an essential role in stabilizing the peak power of TRFL. In this study, the effect of RBS has been proven to flatten the peak power among the generated multiwavelength lasers. The adjustment of the HWP angle does not affect the flatness of TRFL due to the RBS effect introduced in the cavity. The TRFL output power is independent of polarization variation with SMF. The best spectrum is observed at an SOA current of 110 mA and EDFA output power of 18 dBm. The spectral bandwidth of all three lasing wavelengths is about 0.25 nm, with an average ER of 21 dB. Owing to the effect of RBS and IDL, the peak power flatness of 0.9 dB is observed within

the emitted lasers. The generated TRFL has good stability recorded within 120 min; the maximum peak power deviation is 0.24 dB and wavelength deviation of only 0.01 nm.

Author Contributions: Conceptualization, A.A.A.L.; methodology, A.A.A.L., N.M.Y. and A.H.S.; software, S.A.; validation, N.M.Y. and A.H.S.; formal analysis, A.A.A.L.; investigation, A.A.A.L.; resources, N.M.Y.; data curation, E.K.N.; writing—original draft preparation, A.A.A.L.; writing—review and editing, M.A.M., N.M.Y., A.H.S. and F.A.; visualization, N.M.Y. and A.H.S.; supervision, N.M.Y. and A.H.S.; project administration, N.M.Y.; funding acquisition, M.A.M., M.T.A. and N.M.Y. All authors have read and agreed to the published version of the manuscript.

Institutional Review Board Statement: Not applicable.

Informed Consent Statement: Not applicable.

Data Availability Statement: Data applicable in a publicly accessible repository.

Conflicts of Interest: The authors declare no conflict of interest.

References

1. Liu, D.; Ngo, N.; Liu, H. Stable multiwavelength fiber ring laser with equalized power spectrum based on a semiconductor optical amplifier. *Opt. Commun.* **2009**, *282*, 1598–1601. [CrossRef]
2. Lopez-Amo, M.; Leandro, D.; de Miguel, V.; Bravo, M.; Fernández-Vallejo, M.; Perez-Herrera, R.A. Random fiber lasers: Application to fiber optic sensors networks. In Proceedings of the 2017 19th International Conference on Transparent Optical Networks (ICTON), Girona, Spain, 2–6 July 2017.
3. Song, Q.; Xiao, S.; Xu, Z.; Shalaev, V.M.; Kim, Y.L. Random laser spectroscopy for nanoscale perturbation sensing. *Opt. Lett.* **2010**, *35*, 2624–2626. [CrossRef] [PubMed]
4. Olivi, M.; Olivi, G. The physics of lasers. In *Lasers in Endodontics: Scientific Background and Clinical Applications*; Olivi, G., De Moor, R., DiVito, E., Eds.; Springer International Publishing: Cham, Switzerland, 2016; pp. 73–82.
5. Gomes, A.S.; Moura, A.L.; de Araújo, C.B.; Raposo, E.P. Recent advances and applications of random lasers and random fiber lasers. *Prog. Quantum Electron.* **2021**, *78*, 100343. [CrossRef]
6. Churkin, D.V.; Sugavanam, S.; Vatnik, I.D.; Wang, Z.; Podivilov, E.V.; Babin, S.A.; Rao, Y.; Turitsyn, S.K. Recent advances in fundamentals and applications of random fiber lasers. *Adv. Opt. Photon.* **2015**, *7*, 516–569. [CrossRef]
7. Li, M.; Chen, X.; Fujii, T.; Kudo, Y.; Li, H.; Painchaud, Y. Multiwavelength fiber laser based on the utilization of a phase-shifted phase-only sampled fiber Bragg grating. *Opt. Lett.* **2009**, *34*, 1717–1719. [CrossRef] [PubMed]
8. Chen, H.; Gao, S.; Zhang, M.; Zhang, J.; Qiao, L.; Wang, T.; Gao, F.; Hu, X.; Li, S.; Zhu, Y. Advances in random fiber lasers and their sensing application. *Sensors* **2020**, *20*, 6122. [CrossRef] [PubMed]
9. Liang, R. *Biomedical Optical Imaging Technologies: Design and Applications*; Springer Science & Business Media: Berlin/Heidelberg, Germany, 2012.
10. Czajkowski, J.; Prykäri, T.; Alarousu, E.; Palosaari, J.; Myllylä, R. Optical coherence tomography as a method of quality inspection for printed electronics products. *Opt. Rev.* **2010**, *17*, 257–262. [CrossRef]
11. Yang, T.-H.; Chen, C.-W.; Jau, H.-C.; Feng, T.-M.; Wu, C.-W.; Wang, C.-T.; Lin, T.-H. Liquid-crystal random fiber laser for speckle-free imaging. *Appl. Phys. Lett.* **2019**, *114*, 191105. [CrossRef]
12. Fotiadi, A.A. An Incoherent Fibre Laser. *Nat. Photonics* **2010**, *4*, 204. [CrossRef]
13. Ji, Z.; Deng, Y.; Wan, H.; Zhang, Z. Tunable multiwavelength Brillouin random fiber laser. In Proceedings of the 2018 Asia Communications and Photonics Conference (ACP), Hangzhou, China, 26–29 October 2018.
14. Feng, T.; Jiang, M.; Ren, Y.; Wang, M.; Yan, F.; Suo, Y.; Yao, X.S. High stability multiwavelength random erbium-doped fiber laser with a reflecting-filter of six-superimposed fiber-Bragg-gratings. *OSA Contin.* **2019**, *2*, 2526–2538. [CrossRef]
15. Feng, X.; Lu, C.; Tam, H.; Wai, P.; Tang, D.; Guan, B.-O. Mechanism for stable, ultra-flat multiwavelength operation in erbium-doped fiber lasers employing intensity-dependent loss. *Opt. Laser Technol.* **2012**, *44*, 74–77. [CrossRef]

16. Shawki, H.; Kotb, H.; Khalil, D. Single-longitudinal-mode broadband tunable random laser. *Opt. Lett.* **2017**, *42*, 3247–3250. [CrossRef]

17. Xu, Y.; Zhang, L.; Chen, L.; Bao, X. Single-mode SOA-based 1kHz-linewidth dual-wavelength random fiber laser. *Opt. Express* **2017**, *25*, 15828–15837. [CrossRef]

18. Tovar, P.; Ynoquio, H.L.; Temporão, G.; von der Weid, J.P. Longitudinal modes in random feedback fiber lasers. In Proceedings of the CLEO: Science and Innovations 2019, San Jose, CA, USA, 5–10 May 2019.

19. Ahmad, H.; Zulkifli, M.Z.; Jemangin, M.H.; Harun, S.W. Distributed feedback multimode Brillouin–Raman random fiber laser in the S-band. *Laser Phys. Lett.* **2013**, *10*, 055102. [CrossRef]

20. Huang, C.; Dong, X.; Zhang, S.; Zhang, N.; Shum, P.P. Cascaded random fiber laser based on hybrid Brillouin-erbium fiber gains. *IEEE Photon. Technol. Lett.* **2014**, *26*, 1287–1290. [CrossRef]

21. Sugavanam, S.; Zulkifli, M.Z.; Churkin, D.V. Multi-wavelength erbium/Raman gain based random distributed feedback fiber laser. *Laser Phys.* **2015**, *26*, 015101. [CrossRef]

22. Margulis, W.; Das, A.; von der Weid, J.-P.; Gomes, A.S.L. Hybrid electronically addressable random fiber laser. *Opt. Express* **2020**, *28*, 23388–23396. [CrossRef] [PubMed]

23. Liu, Y.; Dong, X.; Jiang, M.; Yu, X.; Shum, P. Multi-wavelength erbium-doped fiber laser based on random distributed feedback. *Appl. Phys. B Laser Opt.* **2016**, *122*, 240. [CrossRef]

24. Pan, H.; Guo, T.; Zhang, A.; Liu, C. Multi-wavelength switchable random fibre laser based on double Sagnac-loop filter. *J. Mod. Opt.* **2021**, *68*, 945–952. [CrossRef]

25. Wang, L.; Dong, X.; Shum, P.P.; Su, H. Tunable erbium-doped fiber laser based on random distributed feedback. *IEEE Photon. J.* **2014**, *6*, 1–5.

26. Pheng, S.; Xiaonan, L.; Wang, Z.; Zhu, Y.; Jiang, Z. Multi-wavelength narrow linewidth random fiber laser based on fiber Bragg grating fabry-perot filter. In Proceedings of the 2020 10th International Conference on Information Science and Technology (ICIST), London, UK, 9–15 September 2020.

27. Zhu, Y.Y.; Zhang, W.L.; Jiang, Y. Tunable Multi-wavelength fiber laser based on random rayleigh back-scattering. *IEEE Photon. Technol. Lett.* **2013**, *25*, 1559–1561. [CrossRef]

28. Sugavanam, S.; Yan, Z.; Kamynin, V.; Kurkov, A.S.; Zhang, L.; Churkin, D.V. Multiwavelength generation in a random distributed feedback fiber laser using an all fiber Lyot filter. *Opt. Express* **2014**, *22*, 2839–2844. [CrossRef] [PubMed]

29. Liu, J.; Tong, Z.; Zhang, W.; Shi, X.; Li, J. Tunable multi-wavelength random distributed feedback fiber laser based on dual-pass MZI. *Appl. Phys. B Laser Opt.* **2021**, *127*, 1–9. [CrossRef]

30. Chen, L.; Ding, Y. Random distributed feedback fiber laser pumped by an ytterbium doped fiber laser. *Optik* **2014**, *125*, 3663–3665. [CrossRef]

31. Leandro, D.; Demiguel-Soto, V.; Lopez-Amo, M. High-resolution sensor system using a random distributed feedback fiber laser. *J. Light. Technol.* **2016**, *34*, 4596–4602. [CrossRef]

32. Zhang, W.L.; Song, Y.B.; Zeng, X.P.; Ma, R.; Yang, Z.J.; Rao, Y.J. Temperature-controlled mode selection of Er-doped random fiber laser with disordered Bragg gratings. *Photon. Res.* **2016**, *4*, 102–105. [CrossRef]

33. Wang, Z.; Yan, P.; Huang, Y.; Tian, J.; Cai, C.; Li, D.; Yi, Y.; Xiao, Q.; Gong, M. An Efficient 4-Kw level random fiber laser based on a tandem-pumping scheme. *IEEE Photon. Technol. Lett.* **2019**, *31*, 817–820. [CrossRef]

34. Zhang, A.; Hao, L.; Geng, B.; Li, D. Investigation of narrow band random fiber ring laser based on random phase-shift Bragg grating. *Opt. Laser Technol.* **2019**, *116*, 1–6. [CrossRef]

35. Popov, S.; Butov, O.; Bazakutsa, A.; Vyatkin, M.; Chamorovskii, Y.; Fotiadi, A. Random lasing in a short Er-doped artificial Rayleigh fiber. *Results Phys.* **2019**, *16*, 102868. [CrossRef]

36. Xu, Y.; Zhang, M.; Lu, P.; Mihailov, S.; Bao, X. Multi-parameter sensor based on random fiber lasers. *AIP Adv.* **2016**, *6*, 095009. [CrossRef]

37. Hu, Z.; Ma, R.; Zhang, X.; Sun, Z.; Liu, X.; Liu, J.; Xie, K.; Zhang, L. Weak feedback assisted random fiber laser from 45°-tilted fiber Bragg grating. *Opt. Express* **2019**, *27*, 3255–3263. [CrossRef] [PubMed]

38. Ali, S.; Al-Khateeb, K.A.S.; Bouzid, B. Comparison of the effect structure on ring and linear cavity lasers of er-doped optical fibers. In Proceedings of the 2008 International Conference on Computer and Communication Engineering, Kuala Lumpur, Malaysia, 13–15 May 2008.

39. Yamashita, S.; Hotate, K. Multiwavelength erbium-doped fibre laser using intracavity etalon and cooled by liquid nitrogen. *Electron. Lett.* **1996**, *32*, 1298–1299. [CrossRef]

40. Graydon, O.; Loh, W.; Laming, R.; Dong, L. Triple-frequency operation of an Er-doped twincore fiber loop laser. *IEEE Photon-Technol. Lett.* **1996**, *8*, 63–65. [CrossRef]

41. Sulaiman, A.; Zamzuri, A.; Hitam, S.; Abas, A.; Mahdi, M. Flatness investigation of multiwavelength SOA fiber laser based on intensity-dependent transmission mechanism. *Opt. Commun.* **2013**, *291*, 264–268. [CrossRef]

42. Sulaiman, A.H.; Yusoff, N.M.; Cholan, N.A.; Mahdi, M.A. Multiwavelength Fiber Laser based on Bidirectional Lyot Filter in Conjunction with Intensity Dependent Loss Mechanism. *Indones. J. Electr. Eng. Comput. Sci.* **2018**, *10*, 840–846. [CrossRef]

43. Sulaiman, A.H.; Ismail, A.; Abdullah, F.; Jamaludin, M.Z.; Mahdi, M.A. Stable and broad multiwavelength generation with the assistance of intensity dependent loss mechanism based on bidirectional SOA. *J. Phys. Conf. Ser.* **2020**, *1593*, 012030. [CrossRef]

44. Quan, M.; Li, Y.; Tian, J.; Yao, Y. Multifunctional tunable multiwavelength erbium-doped fiber laser based on tunable comb filter and intensity-dependent loss modulation. *Opt. Commun.* **2015**, *340*, 63–68. [CrossRef]

45. Zhao, Q.; Pei, L.; Zheng, J.; Tang, M.; Xie, Y.; Li, J.; Ning, T. Switchable multi-wavelength erbium-doped fiber laser with adjustable wavelength interval. *J. Light. Technol.* **2019**, *37*, 3784–3790. [CrossRef]

46. Zulkifli, M.; Tamchek, N.; Latif, A.; Harun, S.; Ahmad, H. Flat output and switchable fiber laser using AWG and broadband FBG. *Opt. Commun.* **2009**, *282*, 2576–2579. [CrossRef]